

Fermi National Accelerator Laboratory

FERMILAB-Pub-95/083-E

CDF

Identification of Top Quarks at CDF Using Kinematic Variables

F. Abe et al.
The CDF Collaboration

*Fermi National Accelerator Laboratory
P.O. Box 500, Batavia, Illinois 60510*

April 1995

Submitted to *Physical Review Letters*

Disclaimer

This report was prepared as an account of work sponsored by an agency of the United States Government. Neither the United States Government nor any agency thereof, nor any of their employees, makes any warranty, express or implied, or assumes any legal liability or responsibility for the accuracy, completeness, or usefulness of any information, apparatus, product, or process disclosed, or represents that its use would not infringe privately owned rights. Reference herein to any specific commercial product, process, or service by trade name, trademark, manufacturer, or otherwise, does not necessarily constitute or imply its endorsement, recommendation, or favoring by the United States Government or any agency thereof. The views and opinions of authors expressed herein do not necessarily state or reflect those of the United States Government or any agency thereof.

Identification of Top Quarks at CDF using Kinematic Variables

Abstract

We have used a kinematic technique to distinguish top quark pair production from background in $p\bar{p}$ collisions at $\sqrt{s} = 1.8$ TeV, applied to 67 pb^{-1} of data. We define a sample of $W + \geq 3$ jet events in which the jets are produced at large angles relative to the incident beams. In this sample, we find an excess of events with large jet transverse energies relative to expectations from background. The excess is consistent with top production; a large fraction of events in this kinematic region contains b jets. We interpret these results as evidence that most of the selected events are from $t\bar{t}$ decay.

The CDF Collaboration

F. Abe,¹⁴ H. Akimoto,³² A. Akopian,²⁷ M. G. Albrow,⁷ S. R. Amendolia,²⁴ D. Amidei,¹⁷
J. Antos,²⁹ C. Anway-Wiese,⁴ S. Aota,³² G. Apollinari,²⁷ T. Asakawa,³² W. Ashmanskas,¹⁵
M. Atac,⁷ P. Auchincloss,²⁶ F. Azfar,²² P. Azzi-Bacchetta,²¹ N. Bacchetta,²¹
W. Badgett,¹⁷ S. Bagdasarov,²⁷ M. W. Bailey,¹⁹ J. Bao,³⁵ P. de Barbaro,²⁶
A. Barbaro-Galtieri,¹⁵ V. E. Barnes,²⁵ B. A. Barnett,¹³ P. Bartalini,²⁴ G. Bauer,¹⁶
T. Baumann,⁹ F. Bedeschi,²⁴ S. Behrends,³ S. Belforte,²⁴ G. Bellettini,²⁴ J. Bellinger,³⁴
D. Benjamin,³¹ J. Benlloch,¹⁶ J. Bensinger,³ D. Benton,²² A. Beretvas,⁷ J. P. Berge,⁷
S. Bertolucci,⁸ A. Bhatti,²⁷ K. Biery,¹² M. Binkley,⁷ D. Bisello,²¹ R. E. Blair,¹
C. Blocker,³ A. Bodek,²⁶ W. Bokhari,¹⁶ V. Bolognesi,²⁴ D. Bortoletto,²⁵ J. Boudreau,²³
G. Brandenburg,⁹ L. Breccia,² C. Bromberg,¹⁸ E. Buckley-Geer,⁷ H. S. Budd,²⁶
K. Burkett,¹⁷ G. Busetto,²¹ A. Byon-Wagner,⁷ K. L. Byrum,¹ J. Cammerata,¹³
C. Campagnari,⁷ M. Campbell,¹⁷ A. Caner,⁷ W. Carithers,¹⁵ D. Carlsmith,³⁴ A. Castro,²¹
D. Cauz,²⁴ Y. Cen,²⁶ F. Cervelli,²⁴ H. Y. Chao,²⁹ J. Chapman,¹⁷ M.-T. Cheng,²⁹

G. Chiarelli,²⁴ T. Chikamatsu,³² C. N. Chiou,²⁹ L. Christofek,¹¹ S. Cihangir,⁷
 A. G. Clark,²⁴ M. Cobal,²⁴ M. Contreras,⁵ J. Conway,²⁸ J. Cooper,⁷ M. Cordelli,⁸
 C. Couyoumtzelis,²⁴ D. Crane,¹ D. Cronin-Hennessy,⁶ R. Culbertson,⁵
 J. D. Cunningham,³ T. Daniels,¹⁶ F. DeJongh,⁷ S. Delchamps,⁷ S. Dell'Agnello,²⁴
 M. Dell'Orso,²⁴ L. Demortier,²⁷ B. Denby,²⁴ M. Deninno,² P. F. Derwent,¹⁷ T. Devlin,²⁸
 M. Dickson,²⁶ J. R. Dittmann,⁶ S. Donati,²⁴ R. B. Drucker,¹⁵ A. Dunn,¹⁷ N. Eddy,¹⁷
 K. Einsweiler,¹⁵ J. E. Elias,⁷ R. Ely,¹⁵ E. Engels, Jr.,²³ D. Errede,¹¹ S. Errede,¹¹ Q. Fan,²⁶
 I. Fiori,² B. Flaughner,⁷ G. W. Foster,⁷ M. Franklin,⁹ M. Frautschi,¹⁹ J. Freeman,⁷
 J. Friedman,¹⁶ H. Frisch,⁵ T. A. Fuess,¹ Y. Fukui,¹⁴ S. Funaki,³² G. Gagliardi,²⁴
 S. Galeotti,²⁴ M. Gallinaro,²¹ M. Garcia-Sciveres,¹⁵ A. F. Garfinkel,²⁵ C. Gay,⁹ S. Geer,⁷
 D. W. Gerdes,¹⁷ P. Giannetti,²⁴ N. Giokaris,²⁷ P. Giromini,⁸ L. Gladney,²²
 D. Glenzinski,¹³ M. Gold,¹⁹ J. Gonzalez,²² A. Gordon,⁹ A. T. Goshaw,⁶ K. Goulianos,²⁷
 H. Grassmann,^{7a} L. Groer,²⁸ C. Grosso-Pilcher,⁵ G. Guillian,¹⁷ R. S. Guo,²⁹ C. Haber,¹⁵
 S. R. Hahn,⁷ R. Hamilton,⁹ R. Handler,³⁴ R. M. Hans,³⁵ K. Hara,³² B. Harral,²²
 R. M. Harris,⁷ S. A. Hauger,⁶ J. Hauser,⁴ C. Hawk,²⁸ E. Hayashi,³² J. Heinrich,²²
 M. Hohlmann,^{1,5} C. Holck,²² R. Hollebeek,²² L. Holloway,¹¹ A. Hölscher,¹² S. Hong,¹⁷
 G. Houk,²² P. Hu,²³ B. T. Huffman,²³ R. Hughes,²⁶ J. Huston,¹⁸ J. Huth,⁹ J. Hylen,⁷
 H. Ikeda,³² M. Incagli,²⁴ J. Incandela,⁷ J. Iwai,³² Y. Iwata,¹⁰ H. Jensen,⁷ U. Joshi,⁷
 R. W. Kadel,¹⁵ E. Kajfasz,^{7a} T. Kamon,³⁰ T. Kaneko,³² K. Karr,³³ H. Kasha,³⁵
 Y. Kato,²⁰ L. Keeble,⁸ K. Kelley,¹⁶ R. D. Kennedy,²⁸ R. Kephart,⁷ P. Kesten,¹⁵
 D. Kestenbaum,⁹ R. M. Keup,¹¹ H. Keutelian,⁷ F. Keyvan,⁴ B. J. Kim,²⁶ D. H. Kim,^{7a}
 H. S. Kim,¹² S. B. Kim,¹⁷ S. H. Kim,³² Y. K. Kim,¹⁵ L. Kirsch,³ P. Koehn,²⁶ K. Kondo,³²
 J. Konigsberg,⁹ S. Kopp,⁵ K. Kordas,¹² W. Koska,⁷ E. Kovacs,^{7a} W. Kowald,⁶
 M. Krasberg,¹⁷ J. Kroll,⁷ M. Kruse,²⁵ T. Kuwabara,³² S. E. Kuhlmann,¹ E. Kuns,²⁸
 A. T. Laasanen,²⁵ N. Labanca,²⁴ S. Lammel,⁷ J. I. Lamoureux,³ T. LeCompte,¹¹
 S. Leone,²⁴ J. D. Lewis,⁷ P. Limon,⁷ M. Lindgren,⁴ T. M. Liss,¹¹ N. Lockyer,²² O. Long,²²
 C. Loomis,²⁸ M. Loreti,²¹ J. Lu,³⁰ D. Lucchesi,²⁴ P. Lukens,⁷ S. Lusin,³⁴ J. Lys,¹⁵
 K. Maeshima,⁷ A. Maghakian,²⁷ P. Maksimovic,¹⁶ M. Mangano,²⁴ J. Mansour,¹⁸

M. Mariotti,²¹ J. P. Marriner,⁷ A. Martin,¹¹ J. A. J. Matthews,¹⁹ R. Mattingly,¹⁶
P. McIntyre,³⁰ P. Melese,²⁷ A. Menzione,²⁴ E. Meschi,²⁴ S. Metzler,²² C. Miao,¹⁷
G. Michail,⁹ S. Mikamo,¹⁴ R. Miller,¹⁸ H. Minato,³² S. Miscetti,⁸ M. Mishina,¹⁴
H. Mitsushio,³² T. Miyamoto,³² S. Miyashita,³² Y. Morita,¹⁴ J. Mueller,²³ A. Mukherjee,⁷
T. Muller,⁴ P. Murat,²⁴ H. Nakada,³² I. Nakano,³² C. Nelson,⁷ D. Neuberger,⁴
C. Newman-Holmes,⁷ M. Ninomiya,³² L. Nodulman,¹ S. Ogawa,³² S. H. Oh,⁶ K. E. Ohl,³⁵
T. Ohmoto,¹⁰ T. Ohsugi,¹⁰ R. Oishi,³² M. Okabe,³² T. Okusawa,²⁰ R. Oliver,²² J. Olsen,³⁴
C. Pagliarone,² R. Paoletti,²⁴ V. Papadimitriou,³¹ S. P. Pappas,³⁵ S. Park,⁷ J. Patrick,⁷
G. Pauletta,²⁴ M. Paulini,¹⁵ L. Pescara,²¹ M. D. Peters,¹⁵ T. J. Phillips,⁶ G. Piacentino,²
M. Pillai,²⁶ K. T. Pitts,⁷ R. Plunkett,⁷ L. Pondrom,³⁴ J. Proudfoot,¹ F. Ptohos,⁹
G. Punzi,²⁴ K. Ragan,¹² A. Ribon,²¹ F. Rimondi,² L. Ristori,²⁴ W. J. Robertson,⁶
T. Rodrigo,^{7a} J. Romano,⁵ L. Rosenson,¹⁶ R. Roser,¹¹ W. K. Sakumoto,²⁶ D. Saltzberg,⁵
L. Santi,²⁴ H. Sato,³² V. Scarpine,³⁰ P. Schlabach,⁹ E. E. Schmidt,⁷ M. P. Schmidt,³⁵
G. F. Sciacca,²⁴ A. Scribano,²⁴ S. Segler,⁷ S. Seidel,¹⁹ Y. Seiya,³² G. Sganos,¹²
A. Sgolacchia,² M. D. Shapiro,¹⁵ N. M. Shaw,²⁵ Q. Shen,²⁵ P. F. Shepard,²³
M. Shimojima,³² M. Shochet,⁵ J. Siegrist,¹⁵ A. Sill,³¹ P. Sinervo,¹² P. Singh,²³ J. Skarha,¹³
K. Sliwa,³³ D. A. Smith,²⁴ F. D. Snider,¹³ T. Song,¹⁷ J. Spalding,⁷ P. Sphicas,¹⁶
L. Spiegel,⁷ A. Spies,¹³ L. Stanco,²¹ J. Steele,³⁴ A. Stefanini,²⁴ K. Strahl,¹² J. Strait,⁷ D.
Stuart,⁷ G. Sullivan,⁵ A. Soumarokov,²⁹ K. Sumorok,¹⁶ J. Suzuki,³² T. Takada,³²
T. Takahashi,²⁰ T. Takano,³² K. Takikawa,³² N. Tamura,¹⁰ F. Tartarelli,²⁴ W. Taylor,¹²
P. K. Teng,²⁹ Y. Teramoto,²⁰ S. Tether,¹⁶ D. Theriot,⁷ T. L. Thomas,¹⁹ R. Thun,¹⁷
M. Timko,³³ P. Tipton,²⁶ A. Titov,²⁷ S. Tkaczyk,⁷ D. Toback,⁵ K. Tollefson,²⁶
A. Tollestrup,⁷ J. Tonnison,²⁵ J. F. de Troconiz,⁹ S. Truitt,¹⁷ J. Tseng,¹³ N. Turini,²⁴
T. Uchida,³² N. Uemura,³² F. Ukegawa,²² G. Unal,²² S. C. van den Brink,²³ S. Vejck,
III,¹⁷ G. Velev,²⁴ R. Vidal,⁷ M. Vondracek,¹¹ D. Vucinic,¹⁶ R. G. Wagner,¹ R. L. Wagner,⁷
J. Wahl,⁵ R. C. Walker,²⁶ C. Wang,⁶ C. H. Wang,²⁹ G. Wang,²⁴ J. Wang,⁵ M. J. Wang,²⁹
Q. F. Wang,²⁷ A. Warburton,¹² G. Watts,²⁶ T. Watts,²⁸ R. Webb,³⁰ C. Wei,⁶ C. Wendt,³⁴
H. Wenzel,¹⁵ W. C. Wester, III,⁷ A. B. Wicklund,¹ E. Wicklund,⁷ R. Wilkinson,²²

H. H. Williams,²² P. Wilson,⁵ B. L. Winer,²⁶ D. Wolinski,¹⁷ J. Wolinski,³⁰ X. Wu,²⁴
J. Wyss,²¹ A. Yagil,⁷ W. Yao,¹⁵ K. Yasuoka,³² Y. Ye,¹² G. P. Yeh,⁷ P. Yeh,²⁹ M. Yin,⁶
J. Yoh,⁷ C. Yosef,¹⁸ T. Yoshida,²⁰ D. Yovanovitch,⁷ I. Yu,³⁵ J. C. Yun,⁷ A. Zanetti,²⁴
F. Zetti,²⁴ L. Zhang,³⁴ W. Zhang,²² and S. Zucchelli²

(CDF Collaboration)

¹ *Argonne National Laboratory, Argonne, Illinois 60439*

² *Istituto Nazionale di Fisica Nucleare, University of Bologna, I-40126 Bologna, Italy*

³ *Brandeis University, Waltham, Massachusetts 02254*

⁴ *University of California at Los Angeles, Los Angeles, California 90024*

⁵ *University of Chicago, Chicago, Illinois 60637*

⁶ *Duke University, Durham, North Carolina 27708*

⁷ *Fermi National Accelerator Laboratory, Batavia, Illinois 60510*

⁸ *Laboratori Nazionali di Frascati, Istituto Nazionale di Fisica Nucleare, I-00044 Frascati, Italy*

⁹ *Harvard University, Cambridge, Massachusetts 02138*

¹⁰ *Hiroshima University, Higashi-Hiroshima 724, Japan*

¹¹ *University of Illinois, Urbana, Illinois 61801*

¹² *Institute of Particle Physics, McGill University, Montreal H3A 2T8, and University of Toronto,*

Toronto M5S 1A7, Canada

¹³ *The Johns Hopkins University, Baltimore, Maryland 21218*

¹⁴ *National Laboratory for High Energy Physics (KEK), Tsukuba, Ibaraki 305, Japan*

¹⁵ *Lawrence Berkeley Laboratory, Berkeley, California 94720*

¹⁶ *Massachusetts Institute of Technology, Cambridge, Massachusetts 02139*

¹⁷ *University of Michigan, Ann Arbor, Michigan 48109*

¹⁸ *Michigan State University, East Lansing, Michigan 48824*

¹⁹ *University of New Mexico, Albuquerque, New Mexico 87131*

²⁰ *Osaka City University, Osaka 588, Japan*

²¹ *Universita di Padova, Istituto Nazionale di Fisica Nucleare, Sezione di Padova, I-35131 Padova, Italy*

- ²² *University of Pennsylvania, Philadelphia, Pennsylvania 19104*
- ²³ *University of Pittsburgh, Pittsburgh, Pennsylvania 15260*
- ²⁴ *Istituto Nazionale di Fisica Nucleare, University and Scuola Normale Superiore of Pisa, I-56100 Pisa, Italy*
- ²⁵ *Purdue University, West Lafayette, Indiana 47907*
- ²⁶ *University of Rochester, Rochester, New York 14627*
- ²⁷ *Rockefeller University, New York, New York 10021*
- ²⁸ *Rutgers University, Piscataway, New Jersey 08854*
- ²⁹ *Academia Sinica, Taipei, Taiwan 11529, Republic of China*
- ³⁰ *Texas A&M University, College Station, Texas 77843*
- ³¹ *Texas Tech University, Lubbock, Texas 79409*
- ³² *University of Tsukuba, Tsukuba, Ibaraki 305, Japan*
- ³³ *Tufts University, Medford, Massachusetts 02155*
- ³⁴ *University of Wisconsin, Madison, Wisconsin 53706*
- ³⁵ *Yale University, New Haven, Connecticut 06511*

PACS number(s) : 14.65 Ha, 13.85 Ni, 13.85 Qk

At the Tevatron Collider, Standard Model top quarks predominantly are produced in pairs, and decay as follows : $t\bar{t} \rightarrow W^+bW^-\bar{b}$, where W is the intermediate vector boson, and b represents a b -quark that generates a hadron jet. Events in which both W s decay leptonically ($W \rightarrow e\nu, \mu\nu$), are called dilepton events. Events in which one W decays leptonically and the other hadronically ($W \rightarrow qq'$, where q and q' represent light quarks), are called “lepton + jet” events. Recently the CDF and D0 experiments reported observation of the top quark based on an excess of dilepton events and lepton + jet events compared to the expected background [1], [2]. In this paper we report the results of a simple technique which selects top production based on the kinematics of the events, i.e. using the transverse energies of the observed jets [3]. Initial results from this approach were reported in [4], but with a data sample from 19.3 pb^{-1} of integrated luminosity compared with 67 pb^{-1} for this study.

The CDF detector is described elsewhere [5]. It features charged particle tracking in a solenoidal magnetic field, surrounded by calorimeters with approximately 4π coverage and muon chambers.

We select candidate $t\bar{t}$ events in the electron or muon + jets channel as follows: Events containing a W that decayed to an electron or muon are selected by requiring an electron with transverse energy $E_T^e > 20 \text{ GeV}$, or a muon with transverse momentum, $P_T^\mu > 20 \text{ GeV}/c$. In addition we require missing transverse energy, $\cancel{E}_T > 25 \text{ GeV}$ (signaling the presence of a neutrino from the W decay), and the transverse mass of the lepton and missing energy, $M_T > 40 \text{ GeV}/c^2$ [6]. We further require that candidate events contain at least three jets with transverse energy $E_T(\text{jet}) > 20 \text{ GeV}$ and with $|\eta(\text{jet})| < 2.0$. The three jets are required to be separated from each other by $\Delta R \geq 0.7$, where ΔR is the distance in the η, ϕ plane. Jets are reconstructed within a cone of radius $R=0.4$ around the calorimeter energy cluster centroid [7]. Jet energies (and therefore \cancel{E}_T) are corrected by a pseudorapidity- and energy-dependent factor, which accounts for calorimeter non-linearity and reduced response at detector boundaries. With these requirements, the sample contains 158 events [8].

The expected jet E_T distributions for top events are computed with the HERWIG Monte Carlo [9] program, as in Ref. [4], using $M_{top}=170$ GeV/ c^2 [10]. The expected $W+$ jets background distributions are computed with the VECBOS Monte Carlo program [11] with $W + 3$ jets matrix elements and HERWIG jet fragmentation. VECBOS predictions are found to be in good agreement with the jet E_T distributions in $W+ \geq 1$ jet, $W+ \geq 2$ jet and $Z+$ jet events, and with the angular distribution of jets in $W+ \geq 2$ jet events [4]. Jets from $t\bar{t}$ decay are expected to be emitted at larger angles (θ) than those from directly produced W s with associated jets. Therefore we select a “signal sample” of $W+ \geq 3$ jet events by requiring all three highest E_T jets to have $|\cos\theta^*(\text{jet})| < 0.7$, where θ^* is the jet polar angle in the rest system of the lepton, \not{E}_T and all jets with $E_T > 15$ GeV [12]. Events which fail the θ^* cut form a background-enriched “control sample”. There are 47 events in the signal sample and 111 in the control sample. Monte Carlo studies indicate that the signal and control samples should contain about the same number of top events, while the contribution from direct $W+$ jet production in the signal sample is expected to be approximately three times smaller than in the control sample. The reduced systematic errors associated with the smaller background should improve the sensitivity of the analysis.

We use the E_T of the second and third highest E_T jets to calculate a “relative likelihood” (L) for each event, as a measure of whether the event is more “top-like” or more “QCD background-like”. The relative likelihood is defined in terms of the Monte Carlo predicted jet E_T distributions $\frac{d\sigma^{t\bar{t}}}{dE_T}$ for $t\bar{t}$ (for a given top mass), normalized to unit area, and the same quantity for direct (QCD) $W+$ jet production.

$$L = \frac{\left(\frac{1}{\sigma^{t\bar{t}}} \frac{d\sigma^{t\bar{t}}}{dE_{T2}}\right) \left(\frac{1}{\sigma^{t\bar{t}}} \frac{d\sigma^{t\bar{t}}}{dE_{T3}}\right)}{\left(\frac{1}{\sigma^{QCD}} \frac{d\sigma^{QCD}}{dE_{T2}}\right) \left(\frac{1}{\sigma^{QCD}} \frac{d\sigma^{QCD}}{dE_{T3}}\right)} \quad (1)$$

[13]. The relative likelihood allows a comparison of each individual event to the expectation for QCD and for top in terms of a single number. When $L > 1$ (i.e. $\ln(L) > 0$) the event is more top-like than QCD-like, and vice versa. We note that this comparison does not

depend on absolute rate predictions but rather depends on differences in the predicted shapes of the jet E_T distributions. In figure 1(a) we show the expected $\ln(L)$ distributions for Monte Carlo $t\bar{t}$ (with $M^{top} = 170 \text{ GeV}/c^2$) and direct $W + \text{jet}$ events in the signal sample. In figure 1(b) we show the data sample. The Monte Carlos predict that $22 \pm 5\%$ of direct $W + \text{jet}$ events will be at $\ln(L) > 0$. However, we observe 25 events at $\ln(L) < 0$ and 22 events at $\ln(L) > 0$. This result is similar to that observed previously with 19.3pb^{-1} of data in [4]. We have evaluated backgrounds from non- W and WW events in the same way as in Ref. [4]. The estimated total number of these events in the signal sample is 8.1 ± 2.0 . These background events are expected to have jet E_T distributions for the second and third highest E_T jet which are softer than the VECBOS prediction for QCD $W + \text{jets}$ production. As a result this background is expected primarily at $\ln(L) < 0$. Conservatively, in what follows we use the QCD background shape to represent the shape of all background.

If we make the conservative assumption that all events at $\ln(L) < 0$ are background and normalize the expected background distribution to the observed events with $\ln(L) < 0$, we expect 7.1 ± 2.1 events at $\ln(L) > 0$ compared to 22 observed. If the entire signal sample were background, then allowing for systematic uncertainties (Q^2 scale in QCD Monte Carlo, jet energy scale as in [4]) we obtain a probability of less than 0.26% that the 47 events of the signal sample would be distributed with at least 22 events at $\ln(L) > 0$.

Figure 2(a) shows the control sample $\ln(L)$ distributions for Monte Carlo $t\bar{t}$ and directly produced $W + \text{jet}$ events. In figure 2(b) we show the $\ln(L)$ distribution of the data. There are 79 events at $\ln(L) < 0$ and 32 at $\ln(L) > 0$.

In order to extract the top content of the sample, we perform a two component fit to the observed signal and control sample $\ln(L)$ distributions using the Monte Carlo predictions for the shape of the $t\bar{t}$ and QCD $\ln(L)$ spectra. For VECBOS we use both the predictions based on $Q^2 = M_W^2$ (harder $E_T(\text{jet})$ spectra) and $Q^2 = \langle P_T \rangle^2$ (softer $E_T(\text{jet})$ spectra); $\langle P_T \rangle$ is the average P_T of all partons in the event. For the signal sample the fit yields 18.0 ± 5.5 (18.8 ± 5.4) top events for $Q^2 = M_W^2$ ($Q^2 = \langle P_T \rangle^2$). The fitted content of $t\bar{t}$

events in the signal sample is consistent with the $t\bar{t}$ production cross section reported in [1]. For the control sample the two component fit yields 0.8 ± 8.1 and 14.5 ± 8.1 top events for $Q^2 = M_W^2$ and $Q^2 = \langle P_T \rangle^2$ respectively. The strong dependence on Q^2 of the estimated top content in the control sample results from the larger background in this sample. The results show that the data are not inconsistent with the expectation that the control sample and signal sample contain a comparable number of $t\bar{t}$ events.

The CDF detector is equipped with a silicon vertex detector (SVX [15]) with which we can measure the impact parameter of charged tracks to a precision of $\simeq 10 \mu\text{m}$. A tagging algorithm [1] identifies b -quark jets by reconstructing their decay vertices and their distances from the primary event vertices (SVX tags). A second technique tags b -quark jets by searching for additional leptons from semileptonic b decay (SLT tags [1]). In figure 1(b) the shaded area indicates events with jets tagged by the SVX or SLT. The darker area indicates events with more than one SVX or SLT tag. There are 13 SVX tags (all at $\ln(L) > 0$) in 8 events compared to 2.80 ± 0.35 (1.37 ± 0.17 for $\ln(L) > 0$) SVX tags expected, if all events were background. In the $\ln(L) > 0$ region, the probability that the observed tags are due to a statistical fluctuation of the background is less than 1×10^{-4} [14]. Using the SLT tagging algorithm, which has worse signal-to-background, we observe 11 SLT tags with an expected background of 5.6 ± 0.8 . In the control sample, we observe 5 SVX tags in 4 events compared to an background estimate of 4.10 ± 0.44 , and 9 SLT compared to an expected background of 8.1 ± 1.2 .

As a consistency check we compare the number of observed SVX tagged events in the signal and control samples with what we expect from the top content of the samples. The top content is estimated from the two component fits to the $\ln(L)$ distributions. Multiplying this by the SVX tagging efficiency [16] and adding the expected tags from background yields the expected number of SVX tagged events. The results of this comparison are shown in Table 1. Predictions are shown for the two different Q^2 choices used to simulate the VECBOS background shapes for the two component fits. The agreement between expected and observed tags is good. We note however that the number of SVX tags observed in the

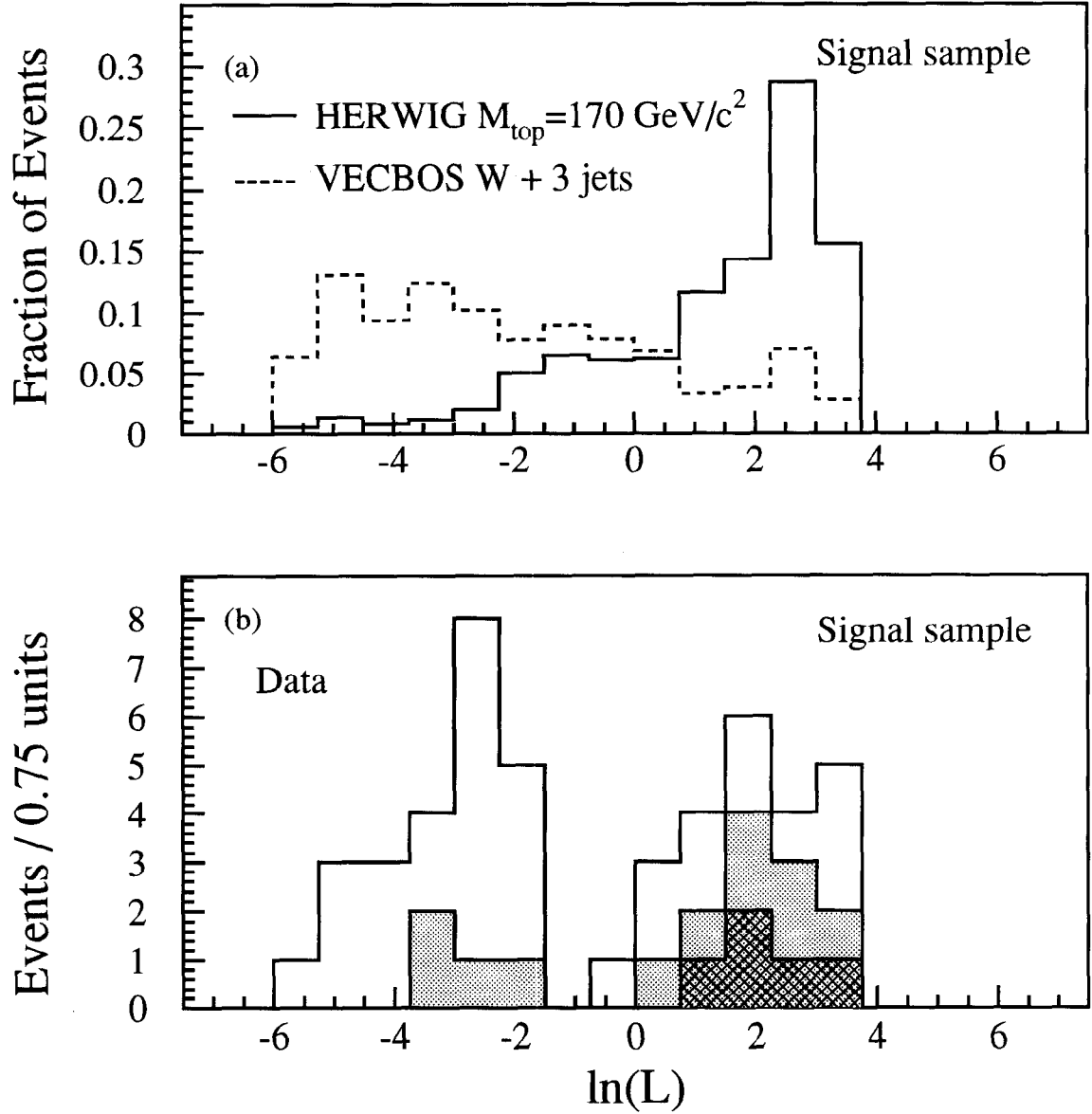


Figure 1: (a) VECBOS QCD and HERWIG ($M_{top} = 170 \text{ GeV}/c^2$) top Monte Carlo predicted distributions for the $W + \geq 3 \text{ jet}$ signal sample. Both distributions are normalized to one; $Q^2 = M_W^2$ is used in the VECBOS calculation; (b) Data; the shaded area indicates the b -tagged events from SVX and SLT; the darker area indicates events with more than one SVX or SLT tag.

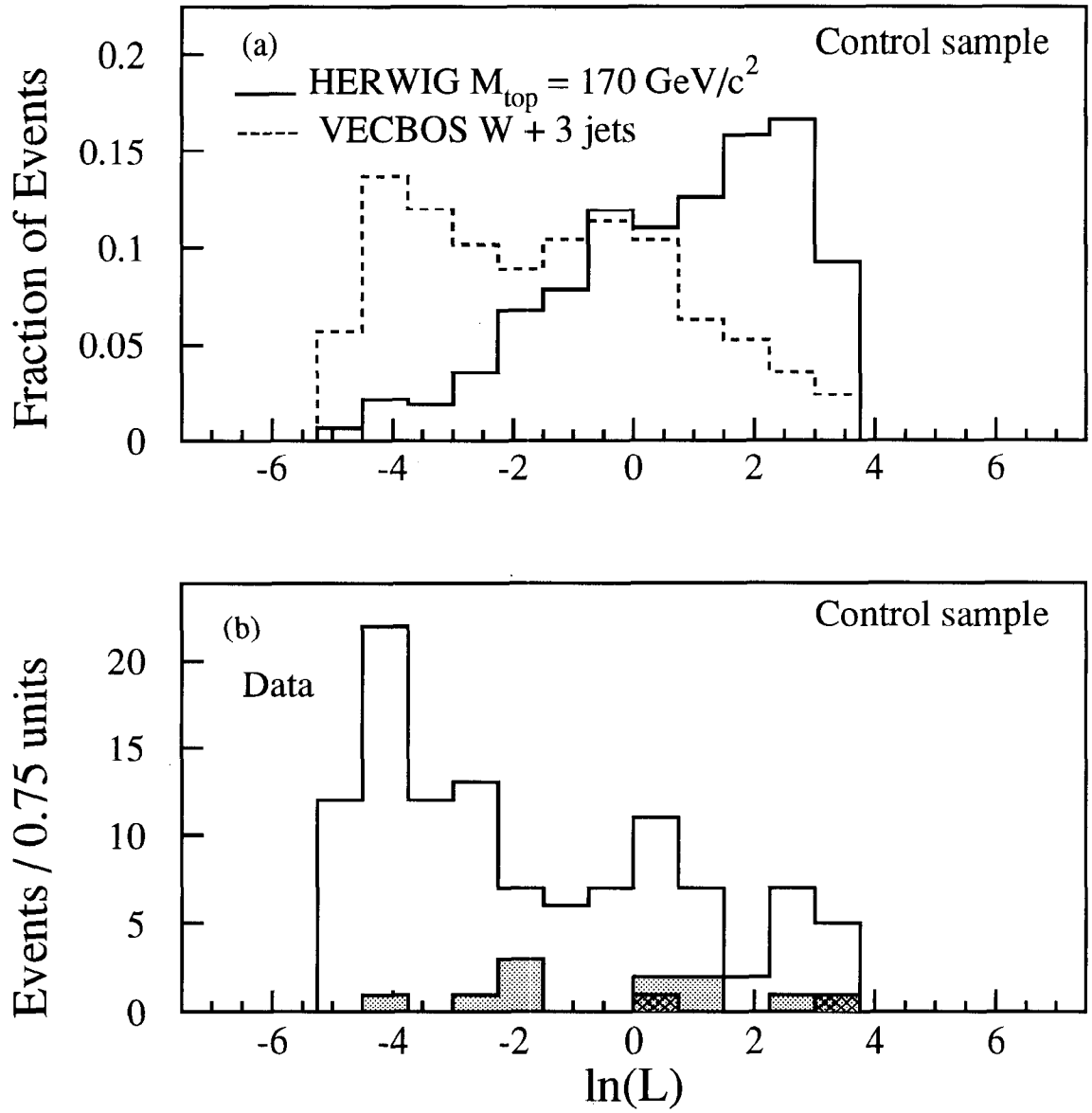


Figure 2: Same as in figure 1, for the control sample.

control sample indicates that the top fraction in this sample may be lower than expected from $t\bar{t}$ Monte Carlo.

Sample	$t\bar{t}$ events from fit	Exp. number of tagged events from backg.	Exp. number of tagged events $t\bar{t}$ + backg.	Observed SVX tagged events
Signal ($Q^2=M_W^2$)	18.0 ± 5.5	1.7 ± 0.2	9.6 ± 2.6	8
Signal ($Q^2=<P_T>^2$)	18.8 ± 5.4	1.7 ± 0.2	10.0 ± 2.6	8
Control ($Q^2=M_W^2$)	0.8 ± 8.1	4.1 ± 0.4	4.4 ± 3.0	4
Control ($Q^2=<P_T>^2$)	14.5 ± 8.1	3.6 ± 0.4	8.8 ± 3.0	4

Table 1: Comparison of the numbers of observed SVX tagged events in the signal and control samples with those expected based on the top content of the samples. The top content is estimated from a two component fit of top and QCD background to the $\ln(L)$ distributions. The expected number of tagged events from background is modified based on the estimated $t\bar{t}$ content of the sample. Comparisons are shown for two different Q^2 choices used to simulate the VECBOS background shapes.

In summary, we observe an excess of events with kinematics as expected for a heavy top quark, compared to direct production of W + jets. We conservatively estimate a probability of less than 0.26% that the 22 events observed at $\ln(L) > 0$ in the signal sample are entirely due to a statistical fluctuation of the background. A large fraction of these events are b -tagged, as expected from top production. The probability that the observed b -tagged events in the kinematically selected “top like” region are due to a background fluctuation is less than 1×10^{-4} [14]. These results confirm the previously reported evidence [4] that $t\bar{t}$ production can be observed using the jet transverse energy distributions of $W + \geq 3$ jet events, and that by appropriate kinematic selection we can obtain a sample of events significantly enriched in $t\bar{t}$.

This work would not have been possible without the skill and hard work of the Fermilab staff. We thank the staffs of our institutions for their many contributions to the construction of the detector. This work is supported by the U.S. Department of Energy, The National Science Foundation, the Natural Sciences and Engineering Research Council of Canada, the Istituto Nazionale di Fisica Nucleare of Italy, the Ministry of Education, Science and Culture of Japan, the National Science Council of the Republic of China, and

the A.P. Sloan Foundation.

References

- [1] F. Abe et al., Phys.Rev.Lett. **74**, 2626 (1995);
F. Abe *et al.*, Phys. Rev. D **50** (1994), 2966;
F. Abe *et al.*, Phys. Rev. Lett. **73** (1994), 225.
- [2] S. Abachi *et al.*, Phys.Rev.Lett **74**, 2632 (1995).
- [3] In the CDF coordinate system, θ is the polar angle with respect to the proton beam direction. The pseudorapidity, η , is defined as $-\ln \tan(\theta/2)$. The transverse momentum of a particle is $P_T = P \sin\theta$. If the magnitude of this vector is obtained using the calorimeter energy rather than the spectrometer momentum, it becomes the transverse energy (E_T). The difference between the vector sum of all the transverse energies in an event and zero is the missing transverse energy (\cancel{E}_T).
- [4] F. Abe et al., “*Kinematic Evidence for top quark pair production at the Tevatron collider*”, FERMILAB-PUB-94/411-E, Phys.Rev.D51;
M. Cobal, PhD Thesis, Univ. Pisa (1994).
- [5] F. Abe et al., Nucl. Instrum. Methods **A271**, 387 (1988).
- [6] The transverse mass M_T is defined as $M_T = [2E_T\cancel{E}_T(1-\cos\Delta\phi)]^{1/2}$, where E_T is the transverse energy of the lepton and $\Delta\phi$ is the difference in azimuthal angle between the missing energy direction and the direction of the lepton.
- [7] The jet cone radius is defined as $R = \sqrt{\Delta\phi^2 + \Delta\eta^2}$, where $\Delta\phi$ is the cone half-width in azimuth and $\Delta\eta$ is the cone half-width in pseudorapidity.
- [8] We note that 98 of these events are in common with the sample of 203 $W + \geq 3$ jet candidates selected in the 1995 paper of reference[1].

- [9] G. Marchesini and B.R. Webber, Nucl. Phys. **B310**, 461 (1988);
G. Marchesini *et al.*, Comput. Phys. Comm. **67**, 465 (1992).
- [10] Although $M_{top}=170 \text{ GeV}/c^2$ was assumed, the results are not very sensitive to the value of M_{top} over a range of assumed top values as wide as $150 \text{ GeV}/c^2 < M_{top} < 220 \text{ GeV}/c^2$ [4].
- [11] F.A. Berends, W.T. Giele, H. Kuif, B. Tausk, Nucl. Phys. **B357**, 32 (1991);
W. Giele, Ph.D. Thesis, Univ.Leiden (1989).
- [12] M. Cöbal, H. Grassmann, S. Leone, Il Nuovo Cimento **107A**, 75 (1994).
- [13] Note that L is not a ratio of probabilities, since E_{T2} and E_{T3} are correlated.
- [14] The probability is conservatively calculated based on observing 8 tagged events with a background estimate of 1.37 ± 0.17 tags. We note the b-tag results are correlated with the results of [1].
- [15] P. Azzi *et al.*, “SVX’, the New CDF Silicon Vertex Detector”, FERMILAB-CONF-94/205-E.
- [16] The SVX tagging efficiency for these events is estimated to be $(44 \pm 5)\%$ for the signal sample and $(36 \pm 4)\%$ for the control sample. The reduced efficiency in the control sample is because of the limited geometrical coverage of the vertex detector.